

Acceleration of the highest energy particles. Lecture 3

D. B. MELROSE

School of Physics, University of Sydney - Sydney NSW 2006, Australia

1. – Introduction

Diffusive shock acceleration (DSA) provides a plausible basis for theories of the acceleration of GCR, and for the relativistic electrons in synchrotron sources such as supernova remnants and active galaxies. However, difficulties are encountered when one considers the acceleration of the highest energy particles, including GCR, EGCR and the highest energy electrons in synchrotron sources, including active galactic nuclei (AGN). A related problem for synchrotron sources is how flat ($\alpha < 0.5$) synchrotron spectra are explained in view of DSA implying $\alpha > 0.5$.

2. – Acceleration of cosmic rays

An explanation of the acceleration of cosmic rays was one of the major objectives for the theory of DSA. The theory works well for the lower energy particles in the GCR component, cf. fig. 1 in Lecture 1 (p. 35), but encounters difficulties at higher energies. The acceleration of the EGCR component remains relatively poorly understood.

2.1. Acceleration of GCR. – An energetic argument suggests that GCRs are accelerated in association with supernova explosions. The energy density in GCRs is approximately 1 eV cm^{-3} . Assuming that they are confined to a volume 10^{68} cm^3 in the galactic disk, the total energy in GCRs is 10^{49} J , and with a lifetime of 10^7 y , the power needed to maintain the observed cosmic ray spectrum is $3 \times 10^{34} \text{ W}$. The most energetic events in the Galaxy are supernova explosions, each of which releases $\sim 10^{45} \text{ J}$ and which occur at a rate of about three per century, giving a power $\sim 10^{36} \text{ W}$. Several per cent of this energy needs to go into GCRs to maintain their spectrum. Acceleration of GCR is now attributed to DSA at strong shocks created by supernovae. The relative abundances

of the elements in GCRI is consistent with them arising from the ISM rather than the progenitor stars of the supernovae. This suggests a multiple-shock model in which the acceleration occurs in the ISM due to the passage of strong shocks from supernovae.

A “leaky-box” model involves DSA at shocks injecting new energetic particles from the ISM, with this injection being balanced by escape of cosmic rays. This model corresponds to

$$(1.1) \quad \frac{\partial f(p)}{\partial t} = Q(p) - \frac{f(p)}{t_{\text{esc}}},$$

where $Q(p) \propto p^{-b}$ describes the acceleration and t_{esc} is an escape time. The steady-state distribution is $f(p) = Q(p)t_{\text{esc}}$. The theory needs to account for the spectral index of GCRI, which is $b = 4.7$. Strong shocks ($r \rightarrow 4$) would produce $b \rightarrow 4$. One possible explanation for the observed spectral index is that the shocks have the compression ratio $r = 2.76$ required for (1.10) in Lecture 2 to give $b = 4.7$. However, this explanation is implausible for the following reason. In a multiple shock model one expects the spectrum to correspond to that of the strongest shocks, and hence one would expect $b \approx 4$. The argument follows from (1.9) in Lecture 2, which implies that if the upstream spectrum is softer than a power law with index b then the downstream spectrum has index b , whereas if the upstream spectrum is harder than a power law with index b then the downstream spectrum has the same index as upstream. As a result the hardest spectrum ultimately dominates. One expects the strongest supernova shock to be strong, $r \rightarrow 4$, so that an index $b \rightarrow 4$ should be expected. Thus one expects $Q(p) \propto p^{-b}$ with $b \rightarrow 4$ in (1.1). However, the steady-state spectrum, $f(p) = Q(p)t_{\text{esc}}$, also includes any p -dependence of t_{esc} . The p -dependence of escape can be estimated from the difference between the spectral index of the primary cosmic rays and of the spallation products, which gives $t_{\text{esc}} \propto p^{-0.6}$. Then $f(p) = Q(p)t_{\text{esc}}$ gives the observed spectrum for $b = 4.1$, consistent with DSA at strong shocks.

The resonant waves required to scatter the cosmic rays may be generated by the cosmic rays themselves for the lower energy GCRI. The cosmic rays are necessarily anisotropic and the small anisotropy causes Alfvén waves to grow with a growth rate given by (1.18) in Lecture 1 (see p. 42). The growth rate is proportional to $k^{1.7}$, and with $k \propto 1/p$ for the resonant waves, this corresponds to $p^{-1.7}$. An estimate of the growth rate due to anisotropy associated with streaming of GCRI through the ISM gives a rate 1/(few hundred y) at $\varepsilon \sim 10^9$ eV. The growth rate for particles near a shock is of the same order of magnitude, suggesting that self-generation of the resonant waves is possible for the lowest energy GCRs. However, the $p^{-1.7}$ of the growth rate implies that there is insufficient time for the resonant waves to grow for energies near or above the knee at $\sim 10^{15}$ eV.

2.2. Scattering by a turbulent spectrum of waves. – Resonant scattering of higher energy GCRs requires an independent source of the resonant waves. An appropriate spectrum of MHD turbulence is required, such that waves with $kR \sim 1$ are present to scatter particles with gyroradius R , cf. (1.6) in Lecture 1. It is known from studies of

scintillations that there is a spectrum of turbulence in the ISM [1]. The spectrum is a power law, with the energy density per unit range of k of the form

$$(1.2) \quad W(k) = \begin{cases} W_0(k/k_0)^{-\rho}, & \text{for } k_0 < k < k_1, \\ 0, & \text{otherwise,} \end{cases}$$

where k_0 and W_0 are constants. The data are compatible with a Kolmogorov spectrum $\rho = 5/3$. The magnetic energy density in the fluctuations is

$$(1.3) \quad \frac{(\delta B)^2}{\mu_0} = \int_{k_0}^{k_1} dk W(k).$$

The specific form of the scattering does not affect the shape of the steady-state spectrum resulting from DSA, but it does limit the maximum energy to which the particles can be accelerated.

2'3. Time available for acceleration. – The maximum energy $\varepsilon_{\max} = p_{\max}c$ is limited by either the time available for acceleration or by the outer scale of the turbulence. The latter condition implies that the acceleration is ineffective for particles with gyroradius $R > 1/k_0$.

The time, T , taken for the particles to be accelerated from an initial value p_0 to p follows from (1.14) in Lecture 2:

$$(1.4) \quad T = \int_{p_0}^{p_{\max}} dp \left(\frac{c\lambda}{u_1^2 p} \right),$$

with $\lambda = \lambda_1 + r\lambda_2$ and where a strong shock, $r = 4$, is assumed. The scattering mean free path follows from $\lambda = 3\kappa/v$ with κ given by (1.20) in Lecture 1 and with the pitch-angle diffusion coefficient given by (1.19) in Lecture 1:

$$(1.5) \quad \lambda = 0.1 \frac{B^2/2\mu_0}{k^2 W(k)},$$

where the numerical coefficient is of little significance. The dependence of λ on p and B is of the form

$$(1.6) \quad \lambda = \lambda_0 \left(\frac{p}{m_e c} \right)^\zeta \left(\frac{B}{B_0} \right)^{-\zeta}, \quad \zeta = 2 - \rho,$$

where $\lambda_0 \propto (\delta B/B)^{-2}$ and B_0 are fiducial values. For a Kolmogorov spectrum one has $\rho = 5/3$, $\zeta = 1/3$, and (1.4) gives $T \propto p^{1/3}$. A restriction on T , which must be less than the lifetime of cosmic rays in the galactic disk for example, then leads to a maximum energy to which the particles can be accelerated.

In practice, the limit imposed by the outer scale of the turbulence is the more restrictive. The outer scale length is thought to be $k_0^{-1} \sim 10^{17} \text{ m} \sim 3 \text{ pc}$, cf. [1], and

then (1.6) in Lecture 1 implies that the maximum energy to which the particles can be accelerated is $\varepsilon \sim 10^{15}$ eV. This coincides roughly with the knee that separates GCRI from GCRII in the spectrum in fig. 1 in Lecture 1. Thus DSA seems to account well for GCRI, and evidently some important change occurs in the acceleration at around the position of the knee.

2.4. Acceleration of GCRII. – The GCRII component extends from $\sim 10^{15}$ eV to $\sim 10^{18}$ eV, with $a = 3.1$, and the isotopic abundances change with increasing energy favoring heavier nuclei. The interpretation of the GCRII component is complicated by two conflicting arguments. On the one hand, the foregoing discussion suggests that the GCRII component cannot be accelerated by shocks in the ISM in a similar fashion to GCRI. DSA seems to be ineffective above the knee, and when combined with the change in isotopic abundances, this suggests that the origin of GCRII might be unrelated to GCRI. On the other hand, the fact that the GCRII component joins on smoothly to the GCRI component seems to require that the two components have a common source [2]. The latter argument is based on the fact that the GCRII component has a larger spectral index than the GCRI component. If GCRII were independent of GCRI, then three separate conditions need to be satisfied at the knee: the GCRI component must cut off there, the GCRII component must start at the same energy, and the spectra must be equal at this energy. This combination of conditions is so implausible as to exclude it. Note that the opposite applies at the ankle, where GCRII joins onto the harder EGCR component, and then the plausible interpretation is that the two components are independent.

There are several different theories for the origin of GCRII, with reacceleration of the GCRI component being perhaps the most favored theory, *e.g.*, [2]. An alternative suggestion is that the GCRII component is accelerated as a supernova shock passes through the wind of the progenitor star [3]. At present, the GCRII component is simply not understood.

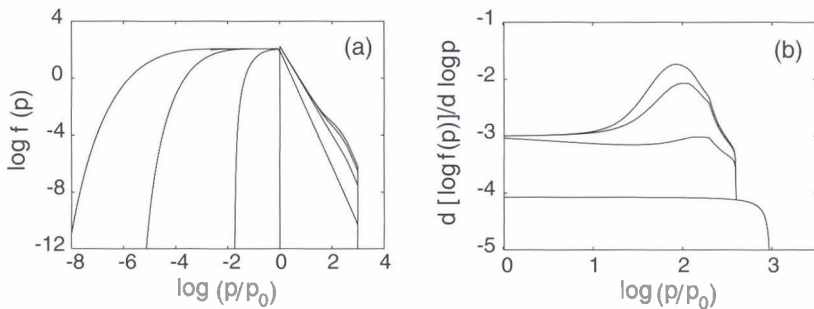


Fig. 1. – The cumulative effect of DSA, injection (at $p = p_0$) at each shock and synchrotron losses in a multiple-shock model [4]: (a) the distribution function and (b) the slope of the distribution function for $p > p_0$. The parameters chosen are $r = 3.8$, $p_c/p_0 = 10^3$ and the plots are for $N = 1, 10, 30, 50$.

3. – Acceleration of extremely high energy electrons

Synchrotron emission is a characteristic signature of relativistic electrons in magnetic fields. It is thought that in most sources the relativistic electrons are accelerated through the DSA. In supernovae and in the knots in some extragalactic jets, there is supporting evidence for the shocks. In the discussion here, emphasis is placed on the effect of synchrotron losses on DSA, in particular on the highest energies that can be achieved and on the spectral index.

3'1. *The effect of synchrotron losses on multiple DSA.* – When synchrotron losses are included as losses, the average acceleration rate (1.14) in Lecture 2 becomes

$$(1.7) \quad \frac{dp}{dt} = Cp - Ap^2, \quad C = \frac{u_1^2}{c\lambda},$$

where the term Ap^2 describes the synchrotron losses, and with λ given by (1.6) for scattering by a turbulent spectrum. No electron can be accelerated to $p > p_c = C/A$.

The effect of synchrotron losses on DSA at multiple shocks is illustrated in fig. 1. It follows that if synchrotron losses determine the maximum energy in DSA, then the distribution becomes harder than $f(p) \propto p^{-4}$, and may even be harder than $f(p) \propto p^{-3}$ at the highest energies [4]. This hardening may be understood in terms of DSA at $p \ll p_c$ driving a flux of electrons in p -space toward higher p and synchrotron losses provide a reflecting barrier at $p = p_c$, where the electrons tend to pile up. Once the spectrum is harder than $f(p) \propto p^{-4}$ synchrotron losses themselves tend to make the spectrum even harder, as illustrated in fig. 2, cf. also [5,6]. Let us consider whether synchrotron losses combined with DSA, can account for the inferred upper cutoff frequency of the synchrotron emission and whether it can explain flat synchrotron spectra.

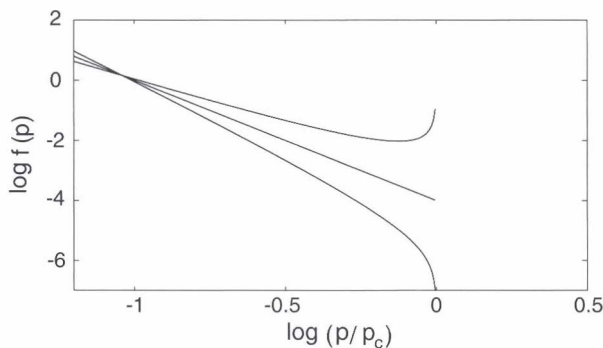


Fig. 2. – The effect of synchrotron losses on initial power law distributions with $b = 3$ (upper curve), $b = 4$ (middle curve) and $b = 5$ (lower curve).

3'2. The synchrotron spectrum of M87. – Detailed observations of extragalactic jets, notably those in M87 and 3C273, show the absence of systematic secular changes in their spectra at all observed scales [7]. The synchrotron spectrum of the jet in M87 is continuous from radio to X-rays, and provides perhaps the strongest constraints on theories for the acceleration of the synchrotron emitting electrons (or positrons) in extragalactic jets. The observational characteristics of the M87 jet include [7]: a) a uniform spectral shape along the jet, $I(\nu) \propto \nu^{-0.6}$, independent of the brightness, and b) a constant upper spectral cutoff of synchrotron electrons at Lorentz factor $\gamma = \gamma_c \approx 0.9 \times 10^6$. The structure of the M87 jet is characterized by several knots, which are interpreted as shocks in the jet flow, and characteristics a) and b) apply both within and between the various knots, down to the smallest resolved scales of ~ 10 pc. The absence of any evidence for spectral evolution associated with synchrotron losses imposes a severe constraint on the acceleration mechanism for the relativistic electrons. The synchrotron half-life at the upper cutoff is [7] $\tau_{\text{syn}}(\gamma_c) = 185(\gamma_c/10^6)^{-1}(B/1\text{T})^{-2}$ y, so that energy losses should affect the spectrum at a distance from an acceleration site ranging from $\lambda_{\text{syn}} = 42$ pc in the inner jet (knot F) to $\lambda_{\text{syn}} = 10$ pc at knot A. These data imply that acceleration must be smoothly distributed along the entire jet, producing an identical particle spectrum $N(\gamma) \propto \gamma^{-2.3}$ with a maximum Lorentz factor, $\gamma_c = 10^6$ everywhere.

3'3. Multiple-shock acceleration and the M87 jet. – DSA at multiple shocks and limited by synchrotron losses is a plausible model for acceleration in jets such as M87 [8]. Numerical modeling of the flow in jets, *e.g.*, [9], suggests a distribution of shocks throughout the jet, with the knots being only the strongest shocks. In order for the spectrum to remain the same along the jet, the time-averaged acceleration must be balanced by the time-averaged synchrotron losses. The acceleration occurs only in the vicinity of each shock, and although synchrotron losses occur everywhere, they are strongly concentrated near the shocks. The power radiated, $\propto \gamma^2 B^2$, in synchrotron emission is much greater, by a factor r^4 , in the compressed magnetic field downstream of a shock than in the uncompressed magnetic field between shocks. Synchrotron losses between shocks is unimportant if the fraction, F , of the volume that is compressed by shocks at any one time satisfies $Fr^4 > 1 - F$. It follows from $\alpha = 0.6$ that one has $b = 4.2$, and then (1.10) in Lecture 2 gives $r = 3.3$ so that $Fr^4 > 1 - F$ requires $F > 5 \times 10^{-3}$. Thus, synchrotron losses between the shocks is unimportant provided a given element of plasma is subjected to shock acceleration for at least 1% of the time.

3'4. Upper energy cutoff. – If the upper energy cutoff, $\gamma_c \approx 10^6$, is attributed to a balance between synchrotron losses and acceleration by DSA in shocks, then the theory needs to account for the observed value and the fact that it does not vary significantly with distance along the jet. The maximum energy is determined by (1.7), giving $m_e c \gamma_c = C/A$. For the particular case where the diffusion is determined by (1.5), one finds

$$(1.8) \quad \gamma_c \approx \left[10^2 \frac{u_1^2}{c^2} \left(\frac{\delta B}{B} \right)^2 \frac{1}{k_0 r_e} \left(\frac{k_0 c}{\Omega_0} \right)^\rho \right]^{1/(3-\rho)} \left(\frac{B}{B_0} \right)^{-\rho/(3-\rho)},$$

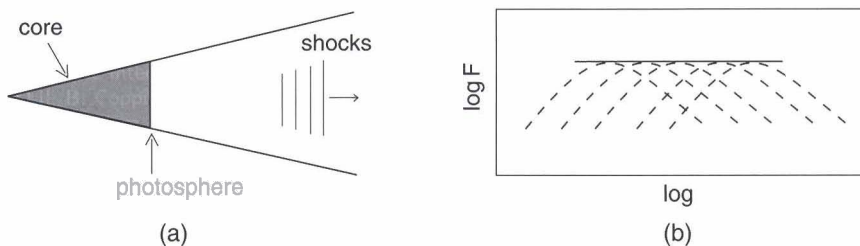


Fig. 3. – The cosmic conspiracy model: (a) the model of an optically thick core that increases in area as the radius r of the jet increases along its length; (b) a flat spectrum results from the locus of the peak of self-absorbed source as it varies such that νr remains constant.

where we are free to choose $k_0 c = \Omega_0$ to determine B_0 in terms of k_0 .

There are two requirements for (1.8) to provide a plausible explanation for the maximum γ inferred for the jet in M87: $\gamma_c \approx 10^6$ and γ_c insensitive to position along the jet. For $u_1 = 10^{-2}c$, $B = 30$ nT, $r_0 = 6 \times 10^4$ m, $(\delta B/B)^2 = 1$ and $L_0 = k_0^{-1}$ we have $k_0 r_0 \approx 2 \times 10^{-12}/L_{0,\text{pc}}$, where $L_{0,\text{pc}}$ is measured L_0 in parsecs, and then $\gamma_c \approx 10^6/L_{0,\text{pc}}^{1/2}$, which for $L_{0,\text{pc}} \approx 1$ is close to the required value. This indicates that a source of turbulence with a characteristic scale 1 pc is required to account $\gamma_c \sim 10^6$ in this way. According to (1.8) with $\rho = 5/3$ and $u_1^2 \propto v_A^2 \propto B^2$, the dependence on B along the jet reduces to $\gamma_c \propto B^{0.1}$, which is clearly very weak. Thus the model seems capable of accounting for both observed features.

3.5. Flat synchrotron spectra. – In the simplest version of DSA, a strong shock results in synchrotron emission with a frequency spectrum $I(\nu) \propto \nu^{-0.5}$, and if the shock is weaker the resulting synchrotron spectrum is steeper, *i.e.* $\alpha > 0.5$. Most synchrotron sources have power law frequency spectra with $\alpha \geq 0.5$, and this fact, together with the evidence for the presence of shocks, has led to wide acceptance of DSA as the primary acceleration mechanism in most synchrotron sources. However, there are some sources that have flatter, $\alpha < 0.5$.

One suggestion for how flat spectra are produced is the “cosmic conspiracy” model illustrated in fig. 3. The jet is assumed to move with constant speed within a cone so that conservation of particles in (1.3) in Lecture 1 implies $K \propto r^{-2}$, where r is the radius of the jet. Assuming that the azimuthal magnetic field dominates, it scales as $B \propto r^{-1}$. The synchrotron emission from optically thin and optically thick portions of the jet then scale as

$$(1.9) \quad F(\nu, r) \propto K B^{1.5} \nu^{-0.5} r^3 \propto (\nu r)^{-0.5}, \quad F(\nu, r) \propto B^{-0.5} \nu^{2.5} r^2 \propto (\nu r)^{2.5},$$

respectively. Both relations (1.9) depend only on the combination νr . Let r_{peak} define the jet radius at which the emitted spectrum peaks at a given ν . If $r_{\text{peak}} \propto 1/\nu$, as (1.9) implies, then it follows that the value of $F(\nu, r)$ at the peak is independent of r and ν , so that the spectrum is flat, as illustrated in fig. 3. Supporting evidence for the cosmic

conspiracy model is provided by evidence that some extragalactic flat spectrum sources are optically thick [10].

An alternative explanation for flat spectra is simply that the acceleration produces an electron spectrum ($b \approx 3$ or $a \approx 1$) which accounts naturally for $\alpha \approx 0$, cf. (1.7) in Lecture 1. The difficulty with this alternative is that the simple theory of DSA results in spectra with $b > 4$. However, there are at least four ways of relaxing the assumptions in the theory to obtain $b < 3$: allow for relativistic shocks with a soft equation of state, allow for oblique rather than parallel shocks, allow for multiple shock acceleration, and assume that the maximum energy in DSA is limited by synchrotron losses. The first two of these have been discussed by Kirk [11], the third is illustrated in fig. 6 in Lecture 2, and the last is illustrated in fig. 1. In particular, DSA at multiple shocks leads naturally to spectra with $b \rightarrow 3$. This suggests that flat spectra should result from multiple DSA whenever synchrotron and other losses between shocks are unimportant. The $b \rightarrow 3$ spectrum then extends to an energy determined by the strength and frequency of the shocks, with a bend to $b \geq 4$ at higher energies.

4. – Acceleration of EGCR

Ultra-high energy cosmic rays (UHECRs) constitute the component of cosmic rays that seems must be of extragalactic origin, that is, the EGCR component in fig. 1 in Lecture 1. The acceleration of these particles is a topic of current active interest. An important constraint on the highest energy particles results from their interaction with photons in the cosmic microwave background (CMB), called the Greisen-Zatsepin-Kuzmin (GZK) effect, see, *e.g.*, [12,13]. Three processes are involved: pair creation $\gamma + Z \rightarrow Z + e^- + e^+$, where Z denotes a nucleus with charge Ze , pion production $\gamma + N \rightarrow N + \pi$, where N denotes a nucleon and π denotes a pion, and photodissociation of nuclei, in which one or more nucleons are knocked out of the nucleus by the photon. In cosmological models the GZK effect becomes of increasing importance with increasing redshift, z , due to the increase in the number density and mean energy of the CMW photons. Possible sources of EGCRs are restricted to relatively nearby cosmological objects (50–100 Mpc) by the GZK effect.

4.1. *Maximum possible energy in SDA and DSA.* – Assuming that EGCRs are accelerated at shocks, the maximum energy to which the particles can be accelerated provides a severe constraint, ruling out most possible shocks. The maximum energy for both SDA and DSA are similar, and the simplest estimate is for SDA at a quasi-perpendicular shock. In this case, the change in magnetic field across the shock implies an electric field, $E = \beta_s cB$, when $\beta_s c$ is related to the shock speed. An effective potential may be estimated by writing $\Phi = EL_s$, where L_s is the maximum extent of the shock. The maximum energy that a particle of charge q can attain is then

$$(1.10) \quad \epsilon_{\max} = |q\Phi| = Ze\beta_s cBL_s.$$

TABLE I. – *The maximum energy for shock acceleration for several examples of shocks in extragalactic sources* [14].

Source	ε_{\max}	D_{\max}	$\langle n \rangle D_{\max}^3$
AGN	10^{16} eV	~ 3 Gpc	10^5
Jets	10^{20} eV	200 Mpc	~ 10
Cocoons	5×10^{19} eV	500 Mpc	~ 100
Clusters	10^{19} eV	1 Gpc	$\sim 10^4$
Superclusters	5×10^{19} eV	500 Mpc	~ 100

For DSA at a parallel shock, one limit on the energy follows from the fact that if the gyroradius of the cosmic ray is too large, it misses the shock. This limit is effectively the same as (1.10).

Various shocks have been suggested as candidates for the acceleration of EGCRs. Table I lists several possible sites in the first column; the second column gives the typical maximum energy ε_{\max} that can be produced there; the third column gives the maximum distance to such a source for which EGCRs could reach the Earth when the redshift due to universal expansion and pion production on the CMB are taken into account; the final column gives the number of sources expected within the sampling volume, estimated from their mean density $\langle n \rangle$ [14]. In the case of clusters, $D_{\max} \sim 1$ Gpc is set by electron-positron pair production on the CMB rather than pion production.

For DSA to be effective for EGCRs, two conditions must be met. First, the acceleration rate must exceed the loss rate due to pion production on the CMB. This limits the energy of particles to

$$(1.11) \quad \varepsilon \leq \varepsilon_{\max, \pi} = \frac{\varepsilon_{\text{tr}}}{\ln(\varepsilon_{\text{tr}}/ZeB\beta_s^2\ell_\pi)},$$

where $\varepsilon_{\text{tr}} \sim 3 \times 10^{20}(1+z)^{-1}$ eV is the threshold energy for pion production and ℓ_π is the loss length due to pion production. Second, the particles must gain more energy at the shock than they lose in transit between shocks. For shocks with a number density n_s and typical size R_s the path length between shocks is $\bar{\ell} \sim 1/n_s\pi R_s^2$. For protons these conditions require [14]

$$(1.12) \quad \beta_s^2 \frac{B}{10^{-6} \text{ G}} \geq 10^{-2}, \quad \Upsilon = n_s \left(\frac{c}{H_0} \right)^3 \geq 10^7 h^{-3} \left(\frac{R_s}{10 \text{ Mpc}} \right)^{-2},$$

where $H_0 = 100h \text{ km s}^{-1} \text{ Mpc}^{-1}$ is the Hubble constant and Υ is the number of shocks per cubic Hubble radius.

There are strong constraints on the type of shock which could be effective in accelerating particles to $> 10^{20}$ eV. For (cosmologically) young shocks, including shocks that

TABLE II. – *Requirements for acceleration of UHECRs at extragalactic shocks* [14]

Object	$\beta_s^2 B/10^{-6} \text{ G}$	$R_s/10 \text{ Mpc}$	Υ
Hot spots	~ 100	10^{-4}	10^5
Cocoons	$\leq 10^{-2}$	10^{-2}	10^5
Quasar bubbles ²	$\sim 10^{-6}$	~ 1	5×10^7
Clusters	$\leq 10^{-6}$	~ 0.5	3×10^5
Superclusters	$\leq 10^{-4}$	~ 3	10^4

are driven continuously, tend to be fast, but small and not very numerous. On the other hand, old shocks such as those associated with fossil quasars or (super)clusters are large, but slow. In either case, for protons simple estimates give the values listed in table II [14]. The table suggests that no object is capable of satisfying both requirements (1.12) for effective acceleration simultaneously.

4.2. *Acceleration of EGCRs in GRBs.* – An alternative suggestion is that EGCRs are accelerated in association with gamma ray bursters (GRBs) [15-17]. The strongest argument in favor of this is a numerical one: if one assumes a comparable efficiency for the production of gamma rays and of UHECRs then the predicted flux of UHCRs from GRBs within 50–100 Mpc matches the observed flux. However, one does not expect the UHCRs to arrive at the same time as the gamma rays: the small deflections by the intergalactic magnetic field do not cause the direction of propagation of the UHECR to change substantially, but they do cause a sufficiently long delay in the propagation time, compared with the light propagation time, to preclude observable correlations.

The fireball model [18] is favored for GRBs. This model involves a relativistic shock with Lorentz factor 10^2 – 10^3 and one suggestion is that the UHECRs are accelerated by such shocks. However, a detailed analysis, analogous to that given above for other shocks, leads to an analogous conclusion: the maximum energy is too low to account for the highest energy EGCRs [19]. Although there are several suggestions on how this difficulty might be overcome, these have yet to be supported by convincing models. Thus, the problem of the origin of the EGCR component remains unsolved.

REFERENCES

- [1] RICKETT B. J., *Annu. Rev. Astron. Astrophys.*, **28** (1990) 561.
- [2] AXFORD W. I., *Astrophys. J. Suppl.*, **90** (1994) 937.
- [3] BIERMANN P. L., *Astron. Astrophys.*, **277** (1993) 691.
- [4] MELROSE D. B. and CROUCH A., *Publ. Astron. Soc. Australia*, **14** (1997) 251.
- [5] MELROSE D. B., *Plasma Astrophysics* (Gordon & Breach, New York) 1980.
- [6] SCHLICKEISER R., *Astron. Astrophys.*, **136** (1984) 227.

- [7] MEISENHEIMER K., RÖSER H.-J. and SCHLÖTELBURG M., *Astron. Astrophys.*, **307** (1996) 61.
- [8] MASSAGLIA S., BODO G. and FERRARI A., *Astron. Astrophys.*, **307** (1996) 997; MICONO M., ZURLO N., MASSAGLIA S., FERRARI A. and MELROSE D., *Astron. Astrophys.*, **349** (1999) 323.
- [9] BODO G., MASSAGLIA S., ROSSI P., ROSNER R., MALAGOLI A. and FERRARI A., *Astron. Astrophys.*, **303** (1995) 281.
- [10] COTTON W. D. *et al.*, *Astrophys. J.*, **238** (1980) L123.
- [11] KIRK J. G., MELROSE D. B. and PRIEST E. R., *Plasma Astrophysics* (Springer-Verlag, Berlin) 1994.
- [12] BEREZINSKIĬ V. S., BULANOV S. V., DOGIEL V. A., GINZBURG V. L. and PTUSKIN V. S., *Astrophysics of Cosmic Rays* (North-Holland) 1990.
- [13] GAISSER T. K., *Cosmic Rays and Particle Physics* (Cambridge University Press) 1990.
- [14] NORMAN C. A., MELROSE D. B. and ACHTERBERG A., *Astrophys. J.*, **454** (1995) 60.
- [15] MILGROM M. and USOV V., *Astrophys. J.*, **449** (1995) L37.
- [16] WAXMAN E., *Phys. Rev. Lett.*, **75** (1995) 386.
- [17] VIETRI M., *Astrophys. J.*, **453** (1995) 883.
- [18] REES M. and MÉSÁROS P., *Astrophys. J.*, **430** (1994) L93.
- [19] GALLANT Y. A. and ACHTERBERG A., *Astron. Astrophys.*, **305** (1999) L6.